Enhancing SSVEP-BCI Performance Under Fatigue State Using Dynamic Stopping Strategy

Yuheng Han, Yufeng Ke, *Member, IEEE*, Ruiyan Wang, Tao Wang, and Dong Ming, *Senior Member, IEEE*

***Abstract*— Steady-state visual evoked potential (SSVEP)-based brain-computer interfaces (BCIs) have emerged as a prominent technology due to their high information transfer rate, rapid calibration time, and robust signal-to-noise ratio. However, a critical challenge for practical applications is performance degradation caused by user fatigue during prolonged use. This work proposes novel methods to address this challenge by dynamically adjusting data acquisition length and updating detection models based on a fatigue-aware stopping strategy. Two 16-target SSVEP-BCIs were employed, one using low-frequency and the other using high-frequency stimulation. A self-recorded fatigue dataset from 24 subjects was utilized for extensive evaluation. A simulated online experiment demonstrated that the proposed methods outperform the conventional fixed stopping strategy in terms of classification accuracy, information transfer rate, and selection time, irrespective of stimulation frequency. These findings suggest that the proposed approach can significantly improve SSVEP-BCI performance under fatigue conditions, leading to superior performance during extended use.**

***Index Terms*— SSVEP, BCIs, dynamic stopping strategy.**

I. Introduction

BRAIN-COMPUTER interfaces (BCIs) enable users to communicate or manipulate external devices using brain signals [1]. Steady-state visual evoked potential (SSVEP) is a periodic electrical signal elicited by repetitive visual stimuli, which induces a strong response in the occipital region at a specific frequency and its harmonics [2]. In recent years, the BCI systems based on SSVEP have been extensively investigated due to their relatively high speed, low hardware cost [3], [4]. Significant advances of SSVEP-BCIs have been made in the fields of text spelling [5], rehabilitation medicine [6], equipment control [7], etc.

In the past decades, there has been rapid evolution in SSVEP-based BCIs. To increase the number of targets, several novel coding methods were proposed [8], [9], [10], [11], [12], [13]. In particular, the joint frequency-phase modulation (JFPM) method has been proven highly efficient for multi-target coding in SSVEP-BCIs [13]. Regarding algorithms, a large number of SSVEP detection methods have been proposed in the past few years, such as canonical correlation analysis (CCA) [14], task-related component analysis (TRCA) [15], task-discriminant component analysis (TDCA) [16], sum of squared correlations (SSCOR) [17], etc.

SSVEP-BCIs have witnessed remarkable advancements, offering a promising approach for communication and control applications. However, several practical challenges remain to be addressed for widespread adoption. A critical concern is user fatigue associated with prolonged SSVEP-BCI use. Factors such as high stimulus intensity, overstimulation, and sustained attentional demands can readily induce fatigue in users. Existing research demonstrates a correlation between visual fatigue and reduced cortical excitability, potentially impacting SSVEP-BCI performance [18]. The presence of fatigue resulted in a decrease in both the amplitude and signal-to-noise ratio (SNR) of SSVEP, leading to poor performance in BCI [19]. Therefore, the fatigue state significantly effects the performance of SSVEP-BCI systems during long-term use. Researchers have put great effort into avoiding the effects of visual fatigue on SSVEP-BCIs in recent years, which mainly focused on the stimulus paradigms and target recognition algorithms. It has been found that a comfortable stimulation paradigm can effectively reduce visual fatigue. Siribunyaphat et al. proposed a quick response code for visual stimulus patterns that reduced visual fatigue and outperformed checkboard patterns [20]. Sakurada et al. suggested that using flickering visual stimuli at frequencies greater than the critical flicker frequency could significantly reduce participants' subjective discomfort and fatigue [21]. Concerning algorithms, Gao et al. developed an adaptive optimal-Kernel

Manuscript received 10 November 2023; revised 4 March 2024; accepted 12 March 2024. Date of publication 22 March 2024; date of current version 1 April 2024. This work was supported in part by the National Key Research and Development Program of China under Grant 2021YFF1200603 and in part by the National Natural Science Foundation of China under Grant 62276184 and Grant 61806141. *(Corresponding author: Yufeng Ke.)*

This work involved human subjects or animals in its research. Approval of all ethical and experimental procedures and protocols was granted by the ethics committee of Tianjin University under Application No. TJUE-2022-189.

The authors are with the Academy of Medical Engineering and Translational Medicine, Tianjin University, Tianjin 300072, China, and also with the Haihe Laboratory of Brain-Computer Interaction and Human-Machine Integration, Tianjin 300392, China (e-mail: clarenceke@tju.edu.cn; richardming@tju.edu.cn).

This article has supplementary downloadable material available at https://doi.org/10.1109/TNSRE.2024.3380635, provided by the authors.

Digital Object Identifier 10.1109/TNSRE.2024.3380635

time-frequency representation complex network method to analyze the effects of fatigue on the SSVEP classification accuracy from the perspective of brain networks [22]. Later, they proposed an alternative approach, combining the multivariate empirical mode decomposition with the support vector machine, to improve the detection of SSVEPs under fatigue state [23]. Ajami et al. employed the least absolute shrinkage and selection operator algorithm for frequency recognition and successfully compensated for the fatigue effect [24]. In summary, the improvements in the stimulus paradigms can mitigate visual fatigue, whereas the improvements in the recognition algorithms could ensure accuracy even when the subjects are already fatigued.

Conventional studies of SSVEP-based BCIs fix the time of selection for each trial. However, the optimal duration, which affects the performance of BCIs, might be different for each trial due to many factors such as the non-stationarity of EEG, subject attention level, etc. Therefore, adjusting the time of selection (or the stimulation duration) adaptively for each trial is considered an acceptable solution for effectively improving the performance of SSVEP-BCIs. More recently, dynamic stopping (DS) strategy has been developed to improve the performance of BCIs with short data lengths. By adaptively minimizing the data length used for the classification of each trial, the DS strategy could get a credible output dynamically [25]. Compared to the fixed stopping (FS) strategy with the same duration for each trial, the DS strategy improves the speed of target selection by BCI users and ensures the accuracy of recognition at the same time, which had been demonstrated in previous SSVEP-BCIs studies [26], [27], [28]. Mainsah et al. tested DS strategy in participants with amyotrophic lateral sclerosis, which demonstrated a significant increase in communication rate [25]. Maye et al. developed spatially encoded BCIs using dynamic stopping method, which reduced visual fatigue while maintaining high accuracy [29]. Kalunga et al. exploited a novel algorithm for online SSVEP-based BCI classification based on Riemannian geometry and DS strategy [30]. Wong et al. developed an online adaptive canonical correlation analysis (OACCA) method, which learning the spatial filter from a single trial to multiple trials [31]. Chen et al. proposed a new training-free dynamical optimization algorithm, which significantly improved the performance of online SSVEP-based BCI systems [32].

To address the critical challenge of user fatigue in SSVEP-BCIs, limited research has explored adaptive algorithms. This study proposes two novel fatigue state adaptive approaches based on the DS strategy: the hypothesis testing-based DS strategy and the Bayesian-based DS strategy. Our aim is to improve SSVEP-BCI performance under fatigue conditions. To evaluate their effectiveness, we compared the proposed methods with a conventional fixed-data length (FS) strategy using classification accuracy, selection speed, and information transfer rate (ITR) on an SSVEP fatigue dataset.

II. Method And Materials

A. Participants

Twenty-four healthy adults (twelve males and twelve females, aged 18-26 years) with normal or corrected-to-normal vision participated in the experiment. None of the subjects had a history of neurological disease or had taken any medication or received any medical treatment in the week before the experiment. The Research Ethics Committee of Tianjin University approved the experiment, and each subject was required to read and sign the participant consent form.

B. EEG Recording

The study employed a 64-channel EEG cap for signal acquisition, with the electrodes placed at standard positions of the international 10–20 system. EEG data were recorded using the Synamp2 system (Neuroscan, Inc.) at a sampling rate of 1000 Hz. The frequency passband of the amplifier ranged from 0.15 Hz to 200 Hz. The ground electrode was placed midway between Fz and FPz, while the reference electrode was located on the vertex. Electrode impedances were maintained below 10 KΩ. Event triggers were generated by the computer, sent to the amplifier, and recorded on an event channel synchronized with the EEG data.

C. Experimental Design and Procedure

Participants were instructed to sit 60 cm away from a liquid crystal display (LCD) with a refresh rate of 240 Hz. The stimulus program was developed using the Psychophysics Toolbox extensions [33] in MATLAB (Mathworks, Inc.). Two paradigms were designed to investigate the effects of fatigue on the performance of SSVEP in different frequency bands: a low-frequency stimuli paradigm and a high-frequency stimuli paradigm. To reduce the impact of stimulus factors, we alternated between low-frequency and high-frequency stimuli when designing the experiment. Note that, the terms "low-frequency" and "high-frequency" that are mentioned in this study refer to the relative relationship between the frequency bands of the two stimuli. As shown in Fig. 1, the stimuli coded using the JFPM method [13] was arranged in a 4×4 matrix and displayed at different frequencies (8 Hz to 15.5 Hz or 25.5 Hz to 33 Hz, with an interval of 0.5 Hz) and phases ($0\ \pi$, $0.5\ \pi$, π, and $1.5\ \pi$).

The experiment comprised two portions. The first portion was the training data acquisition experiment, which included 6 blocks of low-frequency visual stimulus and 6 blocks of high-frequency visual stimulus. The second portion was the fatigue experiment, which included 24 blocks of low-frequency visual stimulus and 24 blocks of high-frequency visual stimulus. In each block, there are sixteen trials corresponding to sixteen targets. Every trial consisted of a cue stage and a stimulus stage. First, a green cross was presented for 1 second to indicate the following target stimulus. The subject was instructed to shift gaze point to the target as soon as possible. Then, sixteen stimuli flashed for 2 seconds simultaneously, during which the subject was instructed to gaze at the target stimulus and avoid blinking. In this study, the training experiment data was used to build the classification models for algorithms, while the fatigue experiment data was used to simulate the online experiment testing. The data is available at https://doi.org/10.5281/zenodo.10507229.

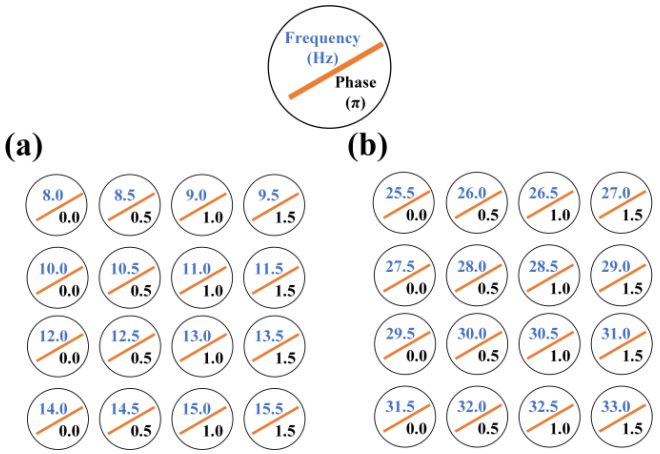

Fig. 1. The layouts of the stimulus frequencies: (a) low-frequency visual stimulus and (b) high-frequency visual stimulus.

D. Data Pre-Processing

Firstly, a 50 Hz notch filter was used to remove common power line noise. Then, eight electrodes (i.e., PO7, PO5, PO3, POz, PO4, PO6, PO8, O1, Oz, and O2) located in parietal and occipital areas were use in following analyses. EEG epochs of each trial were extracted. Considering that the latency delay of the visual pathway is 0.14s [34], the extraction range of the data epoch is [0.14s, 2.14s], where time 0 indicates the beginning of the stimulus.

E. TRCA-Based Method

TRCA is a method that extracts task-related components from neuroimaging data by maximizing reproducibility during task periods [15]. Denote that EEG signals consist of two parts: task-related component $s(t)$ and task-unrelated component $n(t)$. A linear generative model of the multi-channel time signal $x_i(t)$ is assumed as:

$$x_i(t) = a_{1,i} * s(t) + a_{2,i} * n(t), \quad i = 1, \ldots, N_c \tag{1}$$

where i is the index of channels, N_c is the total number of channels, $a_{1,i}$ and $a_{2,i}$ are the mixing coefficients mapping the source signals to the EEG signals. The linear sum of all channel signals is calculated as follows:

$$y(t) = \sum_{i=1}^{N_c} w_i x_i(t) = \sum_{i=1}^{N_c} (w_i a_{1,i} s(t) + w_i a_{2,i} n(t)) \tag{2}$$

By setting $\sum_{i=1}^{N_c} w_i a_{1,i} = 1$ and $\sum_{i=1}^{N_c} w_i a_{2,i} = 0$, We can separate the task-related component $s(t)$ from $y(t)$. This constrained optimization problem can be transformed into a Rayleigh-Ritz eigenvalue problem by Covariance maximization [35]. Similar to filter bank canonical correlation analysis, applying filter bank analysis to TRCA can significantly improve performance [36]. The filter bank analysis is applied to the EEG data for decomposing it into N_k sub-bands. In this study, the k-th sub-band filter for low-frequency stimulus ranges from $k\times 8$ Hz ($k = 1, 2, \ldots, 5$) to 80Hz, whereas the k-th sub-band filter for high-frequency stimulus ranges from $k\times 25.5$ Hz ($k = 1, 2, 3$) to 100Hz. In implementing the band-pass filtering, an additional bandwidth of 2 Hz was added to either side of the passband for each sub-band.

Therefore, the final optimization function is defined as:

$$\hat{w}_n^k = \text{argmax}_w \frac{w^T \boldsymbol{S_n^k} w}{w^T \boldsymbol{Q_n^k} w} \tag{3}$$

where $\boldsymbol{Q} = (Q_{i_1 i_2})_{1\le i_1, i_2 \le N_c}$ in which $Q_{i_1 i_2} = \text{Cov}(x_{i_1}, x_{i_2})$, $\boldsymbol{S} = (S_{i_1 i_2})_{1\le i_1, i_2 \le N_c}$ in which $S_{i_1 i_2} = \sum_{\substack{j_1, j_2 = 1 \\ j_1 \ne j_2}}^{N_t} \text{Cov}(x_{i_1}^{(j_1)}, x_{i_2}^{(j_2)})$, j is the index of trials, N_t is the total number of trials. The optimal solution is the eigenvector of the matrix, whereas the ensemble of all the spatial filters are combined as:

$$\boldsymbol{w^k} = \left[\hat{w}_1^k, \hat{w}_2^k, \ldots, \hat{w}_{N_f}^k\right] \tag{4}$$

where N_f is the total number of targets, $\hat{w}_n^k (n = 1, 2, \ldots, N_f)$ refers to the spatial filtering of the n-th target. The individual training template $\bar{x}_n$ is expressed as:

$$\bar{x}_n^k = \frac{1}{N_t} \sum_i^{N_t} x_{n,i}^k \tag{5}$$

The correlation coefficient between the averaged training data across trials for the n-th target $\bar{x}_n^k$ and the k-th sub-band component of the single-trial test data $\hat{x}^k$ can be calculated as:

$$r_n^k = \rho((\bar{x}_n^k)^T \hat{w}_n^k, (\hat{x})^T \hat{w}_n^k) \tag{6}$$

where $\rho(x, y)$ refers to the Pearson's correlation analysis between two signals x and y. Therefore, the target class can be identified by the following equation:

$$\tau = \underset{n}{\text{argmax}} \sum_{k=1}^{N_k} \left(k^{-a} + b\right) \cdot r_n^k \tag{7}$$

where a and b are set to 1.25 and 0.25.

F. Fatigue State Adaptive Algorithm

Unlike FS strategy, DS strategy adaptively determines the data length used for the classification of each trial. Inspired by this method, we proposed two kinds of fatigue state adaptive algorithms based on DS strategy, which are named hypothesis testing-based DS strategy and Bayesian-based DS strategy. The core idea is to adaptively consider the classification results and recalculate the spatial filter based on the DS strategy. In this way, the data in fatigue state can also be included in the dynamic classification model.

The fatigue state adaptive algorithm consists of an offline training portion and a simulated online testing portion, as shown in Fig. 2. We define two parameters (i.e., a threshold and a judge index) that serve as judging criteria for the algorithm's adaptive updating strategy. Note that, the two kinds of fatigue state adaptive algorithms we proposed above differ only in the way the threshold and the judge index are calculated, which would be described in subsection II-G and subsection II-H, respectively. In the offline training portion, we built the classification model with data length $t = t_0$ (in this study, t_0 is 0.5s and 1s, respectively) and used the

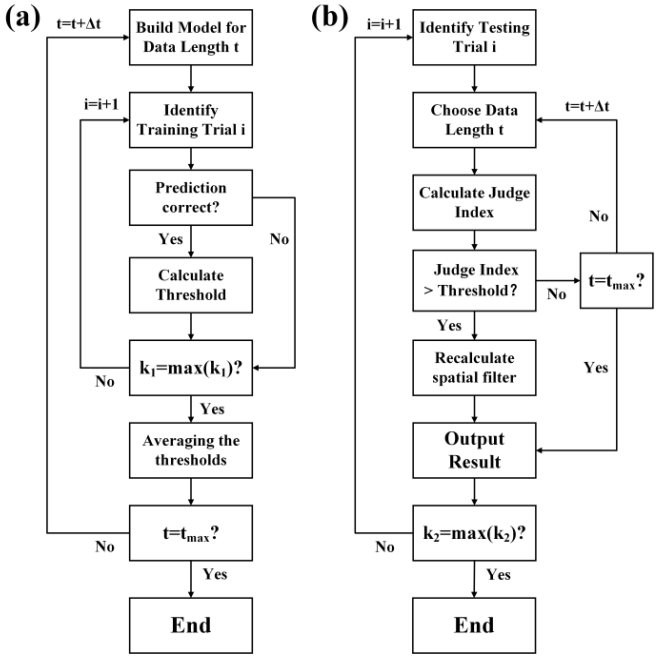

Fig. 2. Diagram of fatigue state adaptive algorithm: (a) offline training flowchart and (b) simulated online testing flowchart.

leave-one-block-out cross-validation method to classify the k_1-th ($k_1 \in [1, 96]$) training trial. If the prediction was correct, the algorithm would calculate and store the threshold, and start classifying the next trial. Otherwise, no threshold would be calculated and the algorithm would proceed the next classification directly. After the classifications of all trials were completed, N_f kinds of target thresholds would be averaged respectively as the threshold for each target classification. To obtain the targets' thresholds at different data lengths, we set the data length $t = t + \Delta t$ ($\Delta t = 0.1$s in this study) and repeated the above procedure until the classification of the data length $t = 2$s was completed. In the simulated online testing portion, we classified the k_2-th ($k_2 \in [1, 384]$) trial with data length $t = t_0$ at the beginning. The judge index of the prediction result was calculated and compared to the corresponding threshold of the prediction target. If the judge index met the criteria of the threshold, the data would be updated into the training dataset to retrain the TRCA-based classification model and update the ensemble spatial filters and the SSVEP templates. Otherwise, the data length t would become $t + \Delta t$ and the data would be re-classified (unless the data length had reached its maximum already). Then, the result would be output and the next trial would be classified. This procedure would be repeated until the classification of all trials had been completed.

G. Hypothesis Testing-Based DS Strategy

Inspired by the main ideas about dynamic windows in Chen et al. 's research [32], we considered the problem of multi-objective SSVEP recognition as a hypothesis-testing problem. In this particular hypothesis-testing problem, the rejection hypothesis indicates that the current data does not convincingly identify a target, and more data needs to be collected. To penalize the most active false predictions, the softmax function was used to establish a projection relation between the metrics calculated by TRCA and the probability distribution. Assuming that the correlation coefficients determined by TRCA-based method can be represented as a vector $\rho = [\rho_1, \rho_2, \ldots, \rho_{N_f}]$, the cost can be expressed by cross-entropy as:

$$Cost\left(H_i\right) = -\sum_{j=1}^{N_f} C\left(H_j, H_i\right) \log \frac{e^{\rho_i}}{\sum_{j=1}^{N_f} e^{\rho_j}}, \quad i = 1, 2, \ldots, N_f \tag{8}$$

where H_i is the result hypothesis. To maximize the distinction between the highest probability hypothesis H_q and the second highest probability hypothesis $H_{q'}$, we defined the function $C\left(H_j, H_q\right)$ as 1 when $j = q$, 0 when $j \neq q$ and $j \neq q'$, and -1 when $j = q'$. In particular, the function $C\left(H_j, H_q\right)$ is an unknown parameter ε when $q = 0$. Therefore, the decision can be made by comparing the cost values of the highest probability hypothesis H_q and the rejection hypothesis H_0. The cost of H_q and H_0 are calculated as follows:

$$Cost\left(H_q\right) = -(\rho_{max} - \rho_{2ndmax}) \tag{9}$$

$$Cost\left(H_0\right) = -\varepsilon\left(\sum_{k=1}^{N_f} \rho_k - N_f \log\left(\sum_{k=1}^{N_f} e^{\rho_k}\right)\right) \tag{10}$$

When $Cost\left(H_0\right)$ is lower than $Cost\left(H_q\right)$, the algorithm believes that there should be more data to identify the target correctly. The comparison can be simplified to:

$$\varepsilon < \frac{(\rho_{max} - \rho_{2ndmax})}{\left(\sum_{k=1}^{N_f} \rho_k - N_f \log\left(\sum_{k=1}^{N_f} e^{\rho_k}\right)\right)} \tag{11}$$

In contrast, if this inequality is not true, the result is considered credible and output. In hypothesis testing-based DS strategy, we denote ε as the threshold, which is calculated by $\frac{Cost(H_q)}{Cost(H_0)}$. In the offline training portion, the algorithm calculates ε for all identified correct trials of each target, and takes the average as the target threshold ε_n, respectively. Thus, the algorithm would obtain N_f thresholds. In the simulated online testing portion, the value of $\frac{Cost(H_q)}{Cost(H_0)}$ in the current data is defined as the judge index ε_{reg}, and compared with the threshold ε_n, which corresponding to the recognition result, to make the classification decision. The result would be output only if $\varepsilon_n \geq \varepsilon_{reg}$.

H. Bayesian-Based DS Strategy

Nakanishi et al. first tested the DS method based on a Bayesian approach in SSVEP-based BCI, and their results suggest the feasibility and efficiency of the DS method [26]. On this basis, Tang et al. enhanced the recognition performance by building respective models for each target [28]. In our study, this method is refined. Fig. 3 shows the key process of Bayesian-based DS strategy. In the offline training portion, we could obtain $N_f \times N_f$ kinds of correlation coefficients calculated by TRCA. We suppose that the correct prediction (i.e., the classification target is identical to the real target) is written as H_1, while the incorrect prediction is written as H_0. We defined r_m as the correlation coefficient

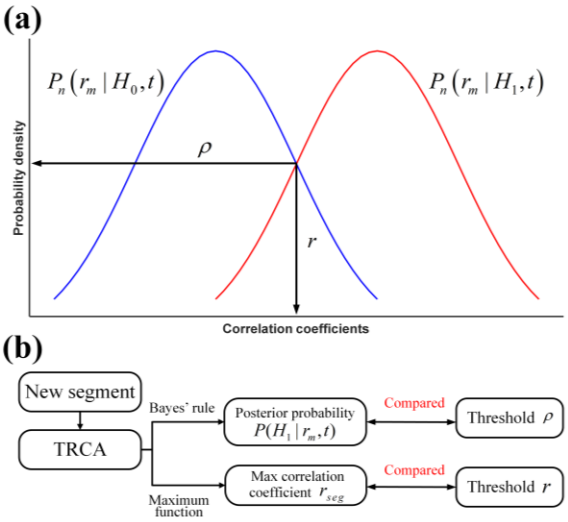

Fig. 3. Key process of Bayesian-based DS strategy: (a) obtain threshold ρ and r through the intersection of H_1's and H_0's pdf, and (b) calculate $P(H_1 \mid r_m, t)$ and r_{seg} and compare to thresholds.

of the real target. The likelihood probability density functions (pdfs) about r_m of H_1 and H_0, $\rho(r_m|H_1,t)$ and $\rho(r_m|H_0,t)$, are generated by Gaussian kernel density estimation respectively, where t indicates the data length used in classification. We considered the probability value ρ and the correlation coefficient r at the intersection of two likelihood pdfs as two thresholds. During the simulated online testing portion, once a new segment has been classified, the posterior probability could be calculated by Bayes' rule as follows:

$$P_n(H_1|r_m,t) = \frac{P_n(r_m|H_1,t)P_n(H_1,t)}{P_n(r_m|H_1,t)P_n(H_1,t) + P_n(r_m|H_0,t)P_n(H_0,t)} \quad (12)$$

where n is the index of the targets, $P_n(H_1,t)$ and $P_n(H_0,t)$ are the prior probabilities of the correct and incorrect prediction generated by the average accuracy and inaccuracy calculated in the offline training portion. We defined the posterior probability $P(H_1|r_m,t)$ and the maximum correlation coefficient of the segment prediction r_{seg} as two judge indices. The algorithm would compare them with the threshold ρ and r. Only if both conditions $P(H_1 \mid r_m,t) > \rho$, and $r_{seg} > r$ are met, Bayesian-based DS strategy would consider the prediction as credible and output it.

I. Performance Evaluation

In this study, we used simulated online testing to evaluate the performance of the proposed methods. The simulated online experiment mimics the process of a real online experiment in which data is collected and processed on a segment-by-segment basis over time. Compared with the real online experiment, the simulated online experiment allows for a fair comparison of different methods on the same data, enabling the identification of the most appropriate method for the online experiment. We choose the accuracy, selection time, and ITR [37] as indicators to measure the performance of different strategies. ITR refers to the number of bits of information transferred per minute. The information quantity B of the target classification can be calculated as:

$$B = \log_2 N_t + p\log_2 p + (1-p)\log_2\left(\frac{1-p}{N-1}\right) \quad (13)$$

where p is the classification accuracy. The ITR is defined as follows:

$$ITR = B \cdot \frac{60}{T} \quad (14)$$

where T is the time required for a selection, including gaze shift time (1s), visual delay (0.14s), and average data length.

TABLE I
OVERALL PERFORMANCE FOR LOW-FREQUENCY SSVEP

Strategy	Data length (s)	Average accuracy (%)	Average ITR (bits·min^{-1})
FS	0.5	83.99±14.17	107.64±30.83
	1	90.23±11.40	93.48±19.04
	2	92.40±10.73	66.77±11.87
Hypothesis testing-based DS	0.5-1	90.64±10.91	111.15±24.44
	1-2	92.69±10.54	84.25±17.60
Bayesian-based DS	0.5-1	89.76±11.26	116.94±25.79
	1-2	92.87±10.54	93.53±17.71

TABLE II
OVERALL PERFORMANCE FOR HIGH-FREQUENCY SSVEP

Strategy	Data length (s)	Average accuracy (%)	Average ITR (bits min^{-1})
FS	0.5	75.48±18.38	90.09±35.42
	1	82.85±17.28	81.20±26.76
	2	87.27±15.20	60.52±16.02
Hypothesis testing-based DS	0.5-1	83.83±16.39	96.68±31.45
	1-2	88.02±14.78	76.75±21.58
Bayesian-based DS	0.5-1	81.42±17.30	99.10±33.69
	1-2	86.69±16.51	83.13±24.40

III. RESULTS

In this section, the TRCA-based FS strategy was selected as a basic target recognition method to detect data with lengths of 0.5s, 1s, and 2s respectively. We compared the performance of Hypothesis testing-based and Bayesian-based DS strategies with the FS strategy.

The comparisons of the classification strategies are summarized in Table I and Table II. For the low-frequency SSVEP-BCI, the highest average accuracies of hypothesis testing-based DS strategy and Bayesian-based DS strategy are 92.68% and 92.87%, whereas the highest average ITRs are 111.15 bits·min^{-1} and 116.94 bits·min^{-1}. For the high-frequency SSVEP-BCI, the highest average accuracies of hypothesis testing-based DS strategy and Bayesian-based DS strategy are 88.02% and 86.69%, whereas the highest average ITRs are 96.68 bits·min^{-1} and 99.10 bits·min^{-1}. In comparison, we find that the results obtained by hypothesis testing-based DS strategy and Bayesian-based DS strategy are more satisfactory compared to those obtained by FS strategy.

In addition, the average accuracy and ITR for all subjects under different data lengths and experimental conditions are

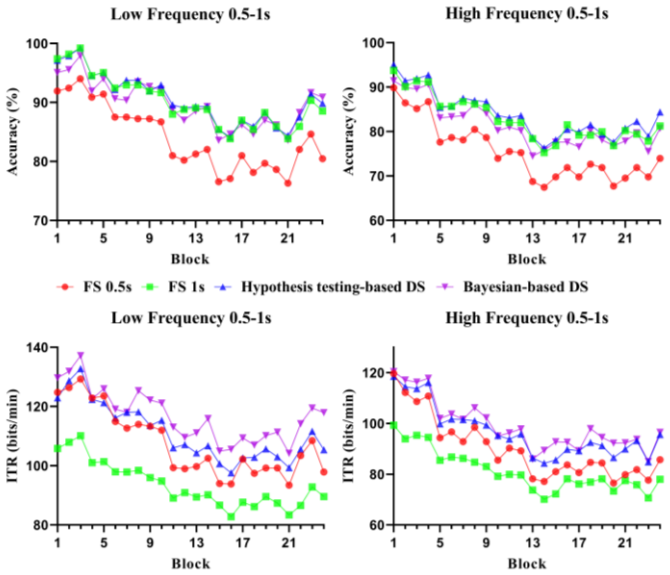

Fig. 4. Accuracy and ITR under different stimulus conditions with data length of 0.5-1s.

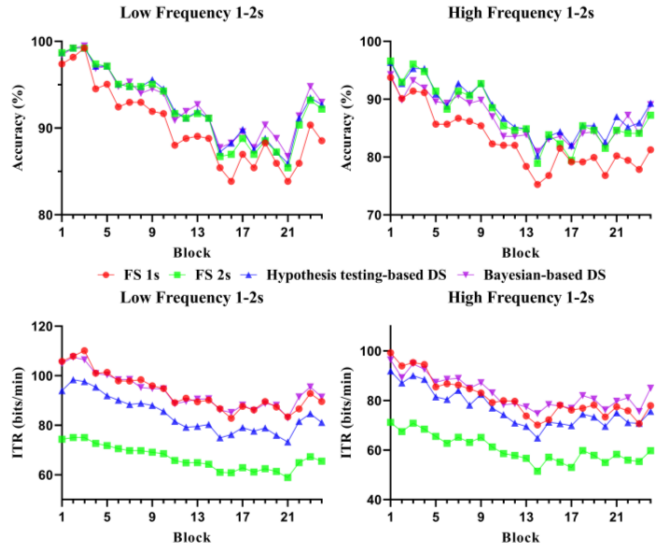

Fig. 5. Accuracy and ITR under different stimulus conditions with data length of 1-2s.

shown in Fig. 4 and Fig. 5. Fig. 4 shows the performance of different methods using 0.5-1s data under different stimuli. The accuracy of each proposed method is close to FS 1s strategy, and much higher than FS strategy with data length of 0.5s, while the ITR of each proposed method is higher than FS strategy with data length of 0.5s, and much higher than FS 1s strategy. These results demonstrate that the two proposed methods could achieve a credible output by adaptively minimizing the data length used, which is the advantage of the DS strategy. Compared to high-frequency stimulus, low-frequency stimulus has higher accuracy and ITR in each block, which is reasonable because low-frequency stimulus could induce a stronger SSVEP response. It is also observed that that as the experiment progressed, both accuracy and ITR tended to decrease due to fatigue with prolonged visual stimulation.

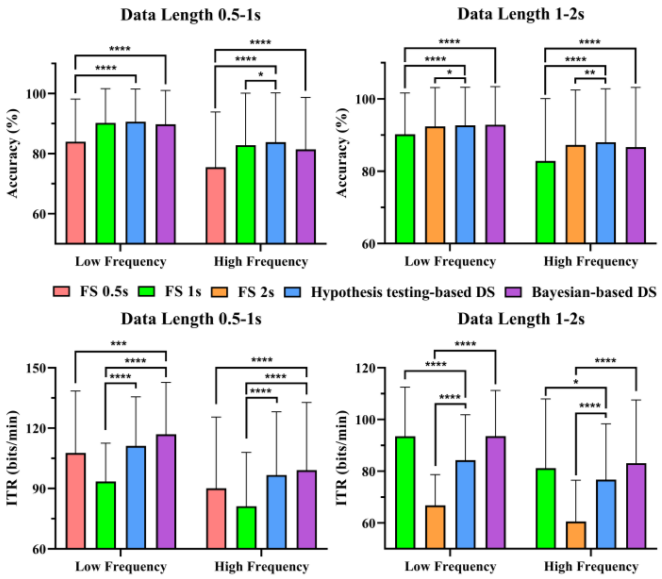

Fig. 6. The overall performance across all the blocks. (∗: p<0.05; ∗∗: p<0.01; ∗ ∗ ∗: p<0.001; ∗ ∗ ∗∗: p<0.0001).

Next, we focus on the results shown in Fig. 5. For accuracy, each proposed method is close to FS 2s strategy and higher than FS 1s strategy. For ITR, Bayesian-based DS strategy shows a considerable result by reaching the level of FS 1s strategy, whereas hypothesis testing-based DS strategy has a poor result. This indicates that hypothesis testing-based DS strategy is too strict in accepting highly credible hypotheses and rejecting less credible ones. Regarding the problem of different stimulus comparisons and the problem of performance degradation caused by fatigue, Fig. 5 differs from Fig. 4 only in the data length, which leads to similar conclusions, so the interpretation would not be repeated.

Then, we performed paired t-tests on the average accuracy and average ITR across all conditions. Relevant performance and statistical analysis results are presented in Supplementary Section A, Tables S1-S8. The overall performance of the simulated online experiment is shown in Fig. 6. In the condition of processing data of length 0.5-1s, statistical analysis shows that the accuracies of DS-based methods are significantly higher than that of FS strategy with data length of 0.5s (hypothesis testing-based: $t_{\text{low}}(23)$=4.850, p_{low} < 0.0001, $t_{\text{high}}(23)$=6.854, p_{high} < 0.0001; Bayesian-based: $t_{\text{low}}(23)$=5.371, p_{low} < 0.0001, $t_{\text{high}}(23)$=6.782, p_{high} < 0.0001) and ITRs DS-based methods are significantly higher than that of FS strategy with 1s data (hypothesis testing-based: $t_{\text{low}}(23)$=12.770, p_{low} < 0.0001, $t_{\text{high}}(23)$=11.270, p_{high} < 0.0001; Bayesian-based: $t_{\text{low}}(23)$=12.110, p_{low} < 0.0001, $t_{\text{high}}(23)$=9.908, p_{high} < 0.0001). It was found that the ITR of the Bayesian-based DS strategy is significantly higher than that of the FS strategy with 0.5s data ($t_{\text{low}}(23)$=4.389, p_{low} = 0.0002, $t_{\text{high}}(23)$=5.105, p_{high} < 0.0001). This is believed to be due to the high accuracy and short selection time guaranteed by the Bayesian-based DS strategy. In the condition of processing data of length 1-2s, statistical analysis shows that the accuracies of the DS-based method are significantly higher than that of FS strategy with 1s data (hypothesis testing-based:

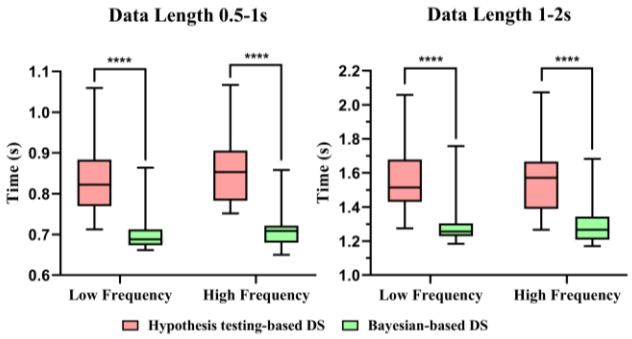

Fig. 7. The selection time of the DS strategies. (∗∗∗∗: p<0.0001).

TABLE III
THE AVERAGE SELECTION TIME UNDER DIFFERENT CONDITIONS

DS strategy	Data length(s)	Frequency range	Selection time (s)
Hypothesis testing-based DS	0.5-1	Low	0.84±0.10
		High	0.86±0.09
	1-2	Low	1.57±0.22
		High	1.58±0.21
Bayesian-based DS	0.5-1	Low	0.71±0.06
		High	0.71±0.04
	1-2	Low	1.30±0.13
		High	1.29±0.11

$t_{low}(23)$=4.805, p_{low} < 0.0001, $t_{high}(23)$=5.421, p_{high} < 0.0001; Bayesian-based: $t_{low}(23)$=4.803, p_{low} < 0.0001, $t_{high}(23)$=6.777, p_{high} <0.0001) and ITR is significantly higher than that of FS strategy with 2s data (hypothesis testing-based: $t_{low}(23)$=11.400, p_{low} < 0.0001, $t_{high}(23)$=10.810, p_{high} < 0.0001; Bayesian-based: $t_{low}(23)$=20.210, p_{low} < 0.0001, $t_{high}(23)$=12.470, p_{high} < 0.0001). However, the ITR of hypothesis testing-based DS strategy is significantly lower than that of FS strategy with 1s data ($t_{low}(23)$=7.645, p_{low} < 0.0001, $t_{high}(23)$=2.245, p_{high} < 0.0001), which is consistent with the conclusion we mentioned above.

To investigate the effect of DS strategy and recognition models update on the performance, we conducted an ablation study on DS and FS strategy (including with and without updating their recognition models). Relevant results and analyses are presented in Supplementary Section B. To sum up, our ablation study reveals that both parts (i.e., dynamic stopping strategy and model updating) of the proposed method contributed to the performance enhancement.

Moreover, we calculated the performance of FS strategy under data lengths of 0.5-2s (with a step of 0.1s) respectively and performed paired t-tests between the FS strategy and the DS strategies. The performance and statistical analysis results demonstrated the validity of our methods as well. Relevant results and analyses are presented in Supplementary Section C.

Fig. 7 shows the selection time under different conditions, whereas the corresponding mean values are shown in Table III. Paired tests indicates that although the difference in average classification accuracy and ITR between the two DS strategies is insignificant, the average selection time of Bayesian-based DS strategy is significantly reduced compared to hypothesis testing-based DS strategy.

IV. DISCUSSION

A. Performance in Real-Time Analysis

This study introduces two methods based on the DS strategy to address the critical challenge of user fatigue in SSVEP-BCIs. These algorithms offer a significant advantage by dynamically adjusting selection time and updating the recognition model. The experimental results demonstrate the effectiveness of the proposed DS methods. They achieve adaptive minimization of trial output time and significantly shorten data length while maintaining high classification accuracy and ITR. Simulated online experiments further confirm that both DS strategies outperform the conventional FS strategy, regardless of stimulus frequency (low or high). This signifies their potential to improve BCI performance during extended use.

However, before real-world application in online SSVEP-BCI systems, several challenges require attention. Firstly, subjects may have difficulty adapting to the unfixed stimulus duration in the DS situation, which could affect the performance of the online SSVEP-BCI. But, the study by Jiang et al. suggests that the improvement effect of the DS strategy may be higher in real online experiments than in simulated ones [27]. Therefore, this issue needs to be further investigated. Secondly, compared to offline SSVEP-BCI, online SSVEP-BCI requires higher temporal resolution to improve real-time performance. Although the computation complexity does not affect the theoretical calculation of the ITR, the time taken to calculate the classification performance and update the models does impact the actual BCI experience. McFarland et al. stated that the gold standard for evaluating BCIs is their effectiveness in real-time, closed-loop online performance [38]. The model updating approach in the proposed methods will result in a significant increase in computational cost. We have calculated the classification time (i.e., the time of recognition and update) for each trial with a single data length and summarized it in Supplementary Section D, Tabel S24. Regarding the results, our methods have an average classification time that is less than the data updating length Δt (i.e., 0.1s). Although the computational complexity of our methods meets the requirements for online performance, further studies are necessary to prove the feasibility in real-time applications.

B. Potential Directions for Further Improvement

Despite the two proposed methods improved the recognition performance of SSVEP-BCI under fatigue state, there are some potential directions for further improvement.

First, the users' EEG changed as the experiment progressed due to fatigue. Although the proposed methods update the spatial filter in TRCA, the parameters of the filter bank do not change accordingly (i.e., not optimized), which affects the recognition results as well. Demir et al. proposed bio-inspired filter banks (BIFBs) to capture frequency selectivity and subject specificity in the feature extraction stage [39]. The results presented in demonstrate the potential of BIFBs for

enhancing SSVEP-BCI performance. Inspired by this promising approach, the integration of BIFBs with the proposed methods has the potential to further improve BCI performance.

Secondly, as shown in Fig. 7, the selection time of hypothesis testing-based DS strategy was significantly longer than that of Bayesian-based DS strategy, regardless of stimulus frequency or data length. According to equations (13) and (14), when the accuracy does not improve significantly with increasing data length, long data length would lead to low ITR. Therefore, the long selection time is the reason that the ITR performance of hypothesis testing-based DS strategy is less than stellar. To address this issue, it might be helpful to reduce the stringency of the threshold and the judge index. Optimizing the criteria of the parameters will be another possible direction to improve our algorithm.

In addition, deep learning (DL) technique has been successfully applied to various classification tasks in SSVEP-BCIs [40], [41], [42], [43]. Combining DL methods with TRCA methods is a promising direction for enhancing the performance of SSVEP-BCIs. Deng et al.developed a novel algorithm named TRCA-Net to enhance SSVEP signal classification, which enjoys the advantages of both the knowledge-based TRCA method and the deep learning-based approach [44]. However, the neural network-based methods require more training data. The transfer learning (TL) strategy transfers shared knowledge from source subjects to target subjects [45], [46]. There are many studies that have confirmed the excellent performance of the TL strategy in SSVEP-BCIs [47], [48], [49]. Combining the DL technique and the TL strategy with our methods may have the potential to improve the performance of SSVEP-BCIs under fatigue state.

V. Conclusion

This paper proposes two novel adaptive algorithms specifically designed to enhance SSVEP recognition performance while considering user fatigue induced by prolonged stimulation. Simulated online testing demonstrates that both proposed methods effectively improve ITR while maintaining high recognition accuracy. Notably, compared to the fixed stop approach, both the hypothesis testing-based DS strategy and the Bayesian-based DS strategy achieve significantly superior performance in terms of recognition accuracy and ITR. In essence, these adaptive methods offer a robust solution for mitigating the influence of user fatigue in SSVEP-BCI applications, leading to superior performance during extended periods of sustained use.

References

[1] J. N. Mak and J. R. Wolpaw, "Clinical applications of brain–computer interfaces: Current state and future prospects," *IEEE Rev. Biomed. Eng.*, vol. 2, pp. 187–199, 2009.

[2] H. Ramoser, J. R. Wolpaw, and G. Pfurtscheller, "EEG-based communication: Evaluation of alternative signal prediction methods—EEG-basierte kommunikation: Evaluierung alternativer methoden zur signalprädiktion," *Biomedizinische Technik/Biomedical Eng.*, vol. 42, no. 9, pp. 226–233, 1997.

[3] F.-B. Vialatte, M. Maurice, J. Dauwels, and A. Cichocki, "Steady-state visually evoked potentials: Focus on essential paradigms and future perspectives," *Prog. Neurobiol.*, vol. 90, no. 4, pp. 418–438, Apr. 2010.

[4] E. Yin, Z. Zhou, J. Jiang, Y. Yu, and D. Hu, "A dynamically optimized SSVEP brain–computer interface (BCI) speller," *IEEE Trans. Biomed. Eng.*, vol. 62, no. 6, pp. 1447–1456, Jun. 2015.

[5] M. Li, D. He, C. Li, and S. Qi, "brain–computer interface speller based on steady-state visual evoked potential: A review focusing on the stimulus paradigm and performance," *Brain Sci.*, vol. 11, no. 4, p. 450, Apr. 2021.

[6] M. Orban, M. Elsamanty, K. Guo, S. Zhang, and H. Yang, "A review of brain activity and EEG-based brain–computer interfaces for rehabilitation application," *Bioengineering*, vol. 9, no. 12, p. 768, Dec. 2022.

[7] Á. Fernández-Rodríguez, F. Velasco-Álvarez, and R. Ron-Angevin, "Review of real brain-controlled wheelchairs," *J. Neural Eng.*, vol. 13, no. 6, Dec. 2016, Art. no. 061001.

[8] C. Jia, X. Gao, B. Hong, and S. Gao, "Frequency and phase mixed coding in SSVEP-based brain–computer interface," *IEEE Trans. Biomed. Eng.*, vol. 58, no. 1, pp. 200–206, Jan. 2011.

[9] Y. Zhang, P. Xu, T. Liu, J. Hu, R. Zhang, and D. Yao, "Multiple frequencies sequential coding for SSVEP-based brain–computer interface," *PLoS ONE*, vol. 7, no. 3, Mar. 2012, Art. no. e29519.

[10] M. Xu et al., "A visual parallel-BCI speller based on the time–frequency coding strategy," *J. Neural Eng.*, vol. 11, no. 2, Apr. 2014, Art. no. 026014.

[11] Y. Li, J. Pan, F. Wang, and Z. Yu, "A hybrid BCI system combining P300 and SSVEP and its application to wheelchair control," *IEEE Trans. Biomed. Eng.*, vol. 60, no. 11, pp. 3156–3166, Nov. 2013.

[12] M. Xu, H. Qi, B. Wan, T. Yin, Z. Liu, and D. Ming, "A hybrid BCI speller paradigm combining P300 potential and the SSVEP blocking feature," *J. Neural Eng.*, vol. 10, no. 2, Apr. 2013, Art. no. 026001.

[13] X. Chen, Y. Wang, M. Nakanishi, T.-P. Jung, and X. Gao, "Hybrid frequency and phase coding for a high-speed SSVEP-based BCI speller," in *Proc. 36th Annu. Int. Conf. IEEE Eng. Med. Biol. Soc.*, Aug. 2014, pp. 3993–3996.

[14] G. Bin, X. Gao, Z. Yan, B. Hong, and S. Gao, "An online multi-channel SSVEP-based brain–computer interface using a canonical correlation analysis method," *J. Neural Eng.*, vol. 6, no. 4, Aug. 2009, Art. no. 046002.

[15] X. Chen, Y. Wang, M. Nakanishi, X. Gao, T.-P. Jung, and S. Gao, "High-speed spelling with a noninvasive brain–computer interface," *Proc. Nat. Acad. Sci. USA*, vol. 112, no. 44, pp. 6058–6067, Nov. 2015.

[16] B. Liu, X. Chen, N. Shi, Y. Wang, S. Gao, and X. Gao, "Improving the performance of individually calibrated SSVEP-BCI by task-discriminant component analysis," *IEEE Trans. Neural Syst. Rehabil. Eng.*, vol. 29, pp. 1998–2007, 2021.

[17] G. R. Kiran Kumar and M. Ramasubba Reddy, "Designing a sum of squared correlations framework for enhancing SSVEP-based BCIs," *IEEE Trans. Neural Syst. Rehabil. Eng.*, vol. 27, no. 10, pp. 2044–2050, Oct. 2019.

[18] T. Cao, F. Wan, C. M. Wong, J. N. da Cruz, and Y. Hu, "Objective evaluation of fatigue by EEG spectral analysis in steady-state visual evoked potential-based brain–computer interfaces," *Biomed. Eng. OnLine*, vol. 13, no. 1, pp. 1–13, Dec. 2014.

[19] Z. Wu, D. Yao, Y. Tang, Y. Huang, and S. Su, "Amplitude modulation of steady-state visual evoked potentials by event-related potentials in a working memory task," *J. Biol. Phys.*, vol. 36, no. 3, pp. 261–271, Jun. 2010.

[20] N. Siribunyaphat and Y. Punsawad, "Steady-state visual evoked potential-based brain–computer interface using a novel visual stimulus with quick response (QR) code pattern," *Sensors*, vol. 22, no. 4, p. 1439, Feb. 2022.

[21] T. Sakurada, T. Kawase, T. Komatsu, and K. Kansaku, "Use of high-frequency visual stimuli above the critical flicker frequency in a SSVEP-based BMI," *Clin. Neurophysiol.*, vol. 126, no. 10, pp. 1972–1978, Oct. 2015.

[22] Z. Gao et al., "An adaptive optimal-kernel time-frequency representation-based complex network method for characterizing fatigued behavior using the SSVEP-based BCI system," *Knowl.-Based Syst.*, vol. 152, pp. 163–171, Jul. 2018.

[23] Z.-K. Gao et al., "Multivariate empirical mode decomposition and multiscale entropy analysis of EEG signals from SSVEP-based BCI system," *Europhys. Lett.*, vol. 122, no. 4, p. 40010, Jul. 2018.

[24] S. Ajami, A. Mahnam, and V. Abootalebi, "An adaptive SSVEP-based brain–computer interface to compensate fatigue-induced decline of performance in practical application," *IEEE Trans. Neural Syst. Rehabil. Eng.*, vol. 26, no. 11, pp. 2200–2209, Nov. 2018.

[25] B. O. Mainsah et al., "Increasing BCI communication rates with dynamic stopping towards more practical use: An ALS study," *J. Neural Eng.*, vol. 12, no. 1, Feb. 2015, Art. no. 016013.

[26] M. Nakanishi, Y. Wang, Y.-T. Wang, and T.-P. Jung, "A dynamic stopping method for improving performance of steady-state visual evoked potential based brain–computer interfaces," in *Proc. 37th Annu. Int. Conf. IEEE Eng. Med. Biol. Soc. (EMBC)*, Aug. 2015, pp. 1057–1060.

[27] J. Jiang, E. Yin, C. Wang, M. Xu, and D. Ming, "Incorporation of dynamic stopping strategy into the high-speed SSVEP-based BCIs," *J. Neural Eng.*, vol. 15, no. 4, Aug. 2018, Art. no. 046025.

[28] J. Tang et al., "Optimizing SSVEP-based BCI system towards practical high-speed spelling," *Sensors*, vol. 20, no. 15, p. 4186, Jul. 2020.

[29] A. Maye, R. Rauterberg, and A. K. Engel, "Instant classification for the spatially-coded BCI," *PLoS ONE*, vol. 17, no. 4, Apr. 2022, Art. no. e0267548.

[30] E. K. Kalunga, S. Chevallier, Q. Barthélemy, K. Djouani, E. Monacelli, and Y. Hamam, "Online SSVEP-based BCI using Riemannian geometry," *Neurocomputing*, vol. 191, pp. 55–68, May 2016.

[31] C. M. Wong et al., "Online adaptation boosts SSVEP-based BCI performance," *IEEE Trans. Biomed. Eng.*, vol. 69, no. 6, pp. 2018–2028, Jun. 2022.

[32] Y. Chen, C. Yang, X. Chen, Y. Wang, and X. Gao, "A novel training-free recognition method for SSVEP-based BCIs using dynamic window strategy," *J. Neural Eng.*, vol. 18, no. 3, Jun. 2021, Art. no. 036007.

[33] D. H. Brainard, "The psychophysics toolbox," *Spatial Vis.*, vol. 10, no. 4, pp. 433–436, 1997.

[34] M. Nakanishi, Y. Wang, Y.-T. Wang, Y. Mitsukura, and T.-P. Jung, "A high-speed brain speller using steady-state visual evoked potentials," *Int. J. Neural Syst.*, vol. 24, no. 6, Sep. 2014, Art. no. 1450019.

[35] H. Tanaka, T. Katura, and H. Sato, "Task-related component analysis for functional neuroimaging and application to near-infrared spectroscopy data," *NeuroImage*, vol. 64, pp. 308–327, Jan. 2013.

[36] H. K. Lee and Y.-S. Choi, "Enhancing SSVEP-based brain–computer interface with two-step task-related component analysis," *Sensors*, vol. 21, no. 4, p. 1315, Feb. 2021.

[37] P. Yuan, X. Gao, B. Allison, Y. Wang, G. Bin, and S. Gao, "A study of the existing problems of estimating the information transfer rate in online brain–computer interfaces," *J. Neural Eng.*, vol. 10, no. 2, Apr. 2013, Art. no. 026014.

[38] D. J. McFarland, D. J. Krusienski, J. Wolpaw, and E. Wolpaw, "BCI signal processing: Feature translation," in *brain–computer Interfaces: Principles and Practice*, vol. 8. New York, NY, USA: Oxford Univ. Press, 2012, pp. 147–165.

[39] A. F. Demir, H. Arslan, and I. Uysal, "Bio-inspired filter banks for frequency recognition of SSVEP-based brain–computer interfaces," *IEEE Access*, vol. 7, pp. 160295–160303, 2019.

[40] C.-C. Chuang, C.-C. Lee, E.-C. So, C.-H. Yeng, and Y.-J. Chen, "Multi-task learning-based deep neural network for steady-state visual evoked potential-based brain–computer interfaces," *Sensors*, vol. 22, no. 21, p. 8303, Oct. 2022.

[41] J. Chen, Y. Zhang, Y. Pan, P. Xu, and C. Guan, "A transformer-based deep neural network model for SSVEP classification," *Neural Netw.*, vol. 164, pp. 521–534, Jul. 2023.

[42] Y. Li, J. Xiang, and T. Kesavadas, "Convolutional correlation analysis for enhancing the performance of SSVEP-based brain–computer interface," *IEEE Trans. Neural Syst. Rehabil. Eng.*, vol. 28, no. 12, pp. 2681–2690, Dec. 2020.

[43] O. B. Guney, M. Oblokulov, and H. Ozkan, "A deep neural network for SSVEP-based brain–computer interfaces," *IEEE Trans. Biomed. Eng.*, vol. 69, no. 2, pp. 932–944, Feb. 2022.

[44] Y. Deng, Q. Sun, C. Wang, Y. Wang, and S. K. Zhou, "TRCA-net: Using TRCA filters to boost the SSVEP classification with convolutional neural network," *J. Neural Eng.*, vol. 20, no. 4, Aug. 2023, Art. no. 046005.

[45] D. Wu, Y. Xu, and B.-L. Lu, "Transfer learning for EEG-based brain–computer interfaces: A review of progress made since 2016," *IEEE Trans. Cognit. Develop. Syst.*, vol. 14, no. 1, pp. 4–19, Mar. 2022.

[46] Z. Wan, R. Yang, M. Huang, N. Zeng, and X. Liu, "A review on transfer learning in EEG signal analysis," *Neurocomputing*, vol. 421, pp. 1–14, Jan. 2021.

[47] P. Yuan, X. Chen, Y. Wang, X. Gao, and S. Gao, "Enhancing performances of SSVEP-based brain–computer interfaces via exploiting inter-subject information," *J. Neural Eng.*, vol. 12, no. 4, Aug. 2015, Art. no. 046006.

[48] Y. Zhang, S. Q. Xie, C. Shi, J. Li, and Z. Zhang, "Cross-subject transfer learning for boosting recognition performance in SSVEP-based BCIs," *IEEE Trans. Neural Syst. Rehabil. Eng.*, vol. 31, pp. 1574–1583, 2023.

[49] C. M. Wong et al., "Inter- and intra-subject transfer reduces calibration effort for high-speed SSVEP-based BCIs," *IEEE Trans. Neural Syst. Rehabil. Eng.*, vol. 28, no. 10, pp. 2123–2135, Oct. 2020.